Chromosome Research 1993, **1**, 93–106

Evidence for a nuclear compartment of transcription and splicing located at chromosome domain boundaries

R. M. Zirbel, U. R. Mathieu, A. Kurz, T. Cremer & P. Lichter

Received 23 February 1993; received in revised form 27 March 1993;
Accepted for publication by M. Schmid 27 March 1993.

The nuclear topography of splicing snRNPs, mRNA transcripts and chromosome domains in various mammalian cell types are described. The visualization of splicing snRNPs, defined by the Sm antigen, and coiled bodies, revealed distinctly different distribution patterns in these cell types. Heat shock experiments confirmed that the distribution patterns also depend on physiological parameters. Using a combination of fluorescence *in situ* hybridization and immunodetection protocols, individual chromosome domains were visualized simultaneously with the Sm antigen or the transcript of an integrated human papilloma virus genome. Three-dimensional analysis of fluorescence-stained target regions was performed by confocal laser scanning microscopy. RNA transcripts and components of the splicing machinery were found to be generally excluded from the interior of the territories occupied by the individual chromosomes. Based on these findings we present a model for the functional compartmentalization of the cell nucleus. According to this model the space between chromosome domains, including the surface areas of these domains, defines a three-dimensional network-like compartment, termed the interchromosome domain (ICD) compartment, in which transcription and splicing of mRNA occurs.

Key words: Chromosome domains, nuclear organization, nuclear transcripts, snRNP distribution

Introduction

Since many fundamental cellular processes take place in the cell nucleus, it has often been assumed to be a highly structured organelle. This view, however, was generally rejected, since light and electron microscopy failed to visualize higher ordered structures except for the nucleolus. Until the late 1960s, microscopic analyses only allowed differentiation between the highly condensed heterochromatin and the less condensed euchromatin.

In 1969 Monneron & Bernhard rediscovered the structure, which was originally described as the silver-stained nuclear body (Ramon y Cajal 1903) and which is today called the 'coiled body' (for review, see Lamond & Carmo-Fonseca 1993). The diameter of these spherical structures varies between 0.1 and 1 μm. Further nuclear bodies have been described and classified according to their morphology (Bouteille *et al.* 1974). In addition, electron microscopy studies revealed nuclear particles, which occur in clusters and may also be part of a loose fibre network (Monneron & Bernhard 1969). These particles are termed 'interchromatin granules,' to reflect their spatial relation to chromatin: they are located in between the chromatin. High resolution electron microscopy also revealed chromatin-associated fibrils, (perichromatin fibrils; Monneron & Bernhard 1969). More recently, the functions of these morphologically defined structures have been disclosed by combinations of indirect immunodetection, *in situ* hybridization and electron as well as light microscopy.

Visualization of major components of the splicing machinery—the U1, U2, U4/U6 and U5 snRNP (small nuclear ribonucleoprotein particles) proteins—by means of indirect immunofluorescence—revealed a wide nuclear distribution and, in addition, a speckled nuclear staining with 20 to 50 speckles consisting of higher snRNP concentrations (Mattioli & Reichlin 1971, Northway & Tan 1972, Lerner *et al.* 1981, Spector *et al.* 1983, Spector 1984, Reuter *et al.* 1984, Bachmann *et al.* 1986, Nyman *et al.* 1986, Verheijen *et al.* 1986). For most of these analyses anti-Sm antibodies were used, which recognize proteins which are common to all splicing snRNPs. The snRNP accumulations are found to co-localize with the interchromatin granules, the perichromatin fibrils or the coiled bodies (Spector *et al.* 1983, Fakan *et al.* 1984, Bachmann *et al.* 1986, Raska *et al.* 1991, Lamond & Carmo-Fonseca 1993). Based on the snRNP distribution patterns, a nuclear network of snRNPs exclusive from the chromatin was postulated (Spector 1990). *In situ* and *in vivo* detection of U1, U2, U4,

R. M. Zirbel, U. R. Mathieu, A. Kurz and P. Lichter (corresponding author) are at the Abt. Organisation komplexer Genome, Deutsches Krebsforschungszentrum, Im Neuenheimer Feld 280, W-6900 Heidelberg, Germany. Tel: (+49) 6221 424609, Fax: (+49) 6221 410 700. T. Cremer is at the Institut für Humangenetik und Anthropologie der Universität, W-6900 Heidelberg, Germany

U5 and U6 snRNAs combined with the detection of various related proteins revealed another specific distribution pattern of snRNPs in HeLa cells: in addition to a general nuclear distribution of U1snRNA and the non-snRNP splicing factor U2AF, a small number of distinct focal concentrations (termed 'foci') of snRNPs were observed consisting of highly enriched U-RNAs and also stained by antibodies recognizing U2AF and m_3G-cap structures (Carmo-Fonseca *et al.* 1991a, 1991b). Possible structural and/or functional relationships between foci and speckles are not clear at present. Some components are found both in speckles and foci, but others are not. For example, the snRNP foci are not stained by antibodies directed against the non-snRNP splicing factor SC35 or the La antigen (Carmo-Fonseca *et al.* 1991b, Huang & Spector 1992), while the snRNP accumulations in the speckles co-localize with SC-35 (Huang & Spector 1992). Immunoelectron microscopy as well as simultaneous antibody staining of the Sm antigen and the coiled body revealed that the Sm foci (but not the speckles) coincide with the coiled bodies (Raska *et al.* 1991, Spector *et al.* 1992, Carmo-Fonseca *et al.* 1993). Thus, the nuclear concentrations of splicing snRNPs detected by means of immunofluorescence are the result of an accumulation in specific nuclear substructures. Such distinct concentrations of nuclear antigens have also been referred to as 'nuclear domains' (see, for example, Ascoli & Maul 1992).

Not only a number of nuclear antigens, but also RNA transcripts have been found to accumulate in the nucleus (Lawrence *et al.* 1989; Raap *et al.* 1991). Following visualization by *in situ* hybridization, these RNA concentrations can be seen as punctate spots or track-like objects. The emerging picture fits well with the previous findings of newly synthesized RNA in perichromatin fibrils (Falcon *et al.* 1984, 1986). Furthermore, the nuclear RNA species could be delineated in preparations of the nuclear matrix (Xing & Lawrence 1991), a chromatin-depleted nucleoskeleton prepared by certain extraction procedures (for review see Berezney 1991). *In situ* hybridization of poly(dT) oligonucleotides delineates patch-like areas in cell nuclei which are assumed to be concentrations of the nuclear fraction of poly-A + RNA (Carter *et al.* 1991). Therefore, they were considered so-called 'transcript domains'. These regions co-localize with splicing snRNPs (Carter *et al.* 1991), and more recently it was shown that one RNA transcript species is preferentially associated with the poly(dA) regions (Xing *et al.* 1993).

Although many structural features of chromatin organization have been revealed by means of biochemistry and electron microscopy, the chromosomal and suprachromosomal organization of genomes remained widely unknown. In contrast to the presumption that the decondensed genomic DNA contained in one chromosome is distributed throughout the nucleus (see, for example, Comings 1980), the DNA of individual chromosomes has been shown to occupy distinct territories (for review see Lichter *et al.* 1991). This was concluded from experiments in which interphase cell nuclei were microirradiated to generate local chromatin damage. Damaged regions were visualized on the chromosomes when the cells reached the subsequent metaphases (Zorn *et al.* 1979, Cremer *et al.* 1982). These territories, also called 'chromosome domains', were visualized directly by means of *in situ* hybridization, first in interspecies somatic hybrid cells (Schardin *et al.* 1985, Manuelidis 1985, Pinkel *et al.* 1986) and later in cells with normal or aberrant chromosome complements (Lichter *et al.* 1988, Cremer *et al.* 1988, Pinkel *et al.* 1988). The term chromosome domain needs to be distinguished from the term chromatin domain, which refers to spatially and functionally defined subchromosomal regions such as DNA loops (Benyajati & Worcel 1976, Paulson & Laemmli 1977).

By analogy to the fact that the r-DNA is localized and transcribed in the nucleolus, where the formation of the ribosome subunits takes place, it has been postulated that other functional compartments exist in cell nuclei (Blobel 1985, Nyman *et al.* 1986, Hochstrasser & Sedat 1987, Spector 1990, Manuelidis 1990, Carter *et al.* 1991). Hutchison and Weintraub (1985) found DNAse hypersensitive sites in the nuclear periphery, and concluded that active RNA-polymerase II genes are preferentially localized in these regions. However, others did not confirm this finding (Manuelidis & Borden 1988). The direct visualization of nuclear components involved in processes which are part of the avenue of gene expression, such as formation of transcription complexes, RNA transcription and post-transcriptional RNA processing, have in general not revealed a predominant localization in the nuclear periphery, although a peripheral localization of some intron sequences was reported (Berman *et al.* 1990).

In order to analyse the spatial relation of structural entities and functionally defined nuclear components, we investigated the three-dimensional arrangement of chromosome domains and splicing snRNPs or RNA transcripts, respectively. Using a combination of *in situ* hybridization and immunodetection protocols, individual chromosome domains were visualized simultaneously with the Sm antigen or the transcript of an integrated human papilloma virus genome. Three-dimensional analysis of the fluorescently stained target regions was performed by confocal laser scanning microscopy, and the data were used to create an integrated model of the spatial organization of the cell nucleus.

Materials and methods

Cells

HeLa cells and CHO cells were cultured in DMEM supplemented with 5% foetal calf serum, penicillin/streptomycin and 2 mM glutamine. Amniotic fluid

cells, foreskin fibroblasts, IARC 307 cells (immortalized B-cell linage), Friend (mouse erythroleukemia) cells, HEL (human erythroleukemia) cells, Colo 320 (colon carcinoma) cells, SKW (Burkitt lymphoma) cells, and Namalwa (Burkitt's lymphoma) cells were cultured in RPMI 1640 supplemented with 15% foetal calf serum, penicillin/streptomycin and glutamine. The different cell lines were kindly provided by Stefan Joos and Michael Pawlita, the foreskin fibroblasts by Rainer Zawatzky (all three DKFZ, Heidelberg, Germany) and the amniotic fluid cells (obtained by diagnostic amniocentesis) by Dieter Hager (Universität Heidelberg, Germany).

Probes

DNA libraries for the painting of human chromosomes (Collins *et al.* 1991) pBS-1, pBS-7, pBS-8, pBS-10, pBS-11, pBS-16, pBS-18 and pBS-20 were generously provided by Joe Gray (UCSF, CA, USA). For the detection of HPV RNA products, we used a cDNA termed I_3 containing the E6* and E7 coding information on a 683 bp *Eco*RI-*Hind*III fragment derived from cDNA H4 (Schneider-Gädicke & Schwarz 1986, Roggenbuck *et al.* 1990) in vector pGEM-3. This clone was kindly provided by Elisabeth Schwarz (DKFZ, Heidelberg, Germany). The primary E6/E7 RNA can be differentially spliced and in HeLa cells only the spliced product E6* is found (Schneider-Gädicke & Schwarz 1986).

Probe DNA was labelled with biotin or digoxigenin by nick-translation as previously described (Lichter *et al.* 1991).

Non-radioactive *in situ* hybridization

Chromosomal *in situ* suppression hybridization was performed as described (Lichter & Cremer 1992) using the pBS-libraries, derived from sorted human chromosomes, as probes and human Cot-1 DNA as competitor. Suspension cells were allowed to adhere on poly L-lysine coated glass slides. Fixation was performed with 4% para-formaldehyde for 10 min at room temperature (RT) and cells were permeabilized with 0.5% Triton X-100 and 0.5% Saponin for 10 min at RT (foreskin fibroblasts were pretreated with 0.1 M HCl for 10 min at RT prior to the treatment with detergents). Denaturation of interphase cells was performed in 70% formamide/2 × SSC/50 mM sodium phosphate pH 7.0 at 73°C for 3 min followed by incubation in 50% formamide/2 × SSC/50 mM sodium phosphate pH 7.0 for 1 min at the same temperature. Labelled probe DNA was heat denatured separately for 5 min at 75°C, incubated at 37°C for 10 min to allow preannealing of repetitive DNA and applied to the specimen. When nuclear RNA was simultaneously visualized, 20 ng of the corresponding labelled cDNA probe was suspended in 5 µl hybridization cocktail, denatured as above, chilled on ice and added to the hybridization solution containing the library probe DNA. Hybridization was allowed to proceed overnight at 37°C. Following post-hybridization washes, sites of hybridization were visualized by incubation with fluoro-chromes (FITC, rhodamine, Texas red) coupled to anti-digoxigenin antibody or avidin.

Detection of cellular antigens by indirect immunofluorescence

Cells were fixed and permeabilized as described above. The snRNPs were detected by indirect immunofluorescence using the monoclonal anti-Sm antibody Y12 (Lerner *et al.* 1981), kindly donated by Joan Steitz (Yale University, CT, USA). The cells were incubated with a 1 : 500 dilution of this antibody in PBS/Tween 20 (0.05%) at 37°C for 45 min. Coilin was detected using the polyclonal rabbit antibody 116.3 (used in a 1 : 200 dilution) generously supplied by Kerstin Bohmann and Angus Lamond (EMBL, Heidelberg, Germany). Following three washes for 10 min in PBS/Tween 20, antibody binding sites were visualized by FITC- or TRITC-conjugated anti-mouse or anti-rabbit antibodies (5 µg/ml), respectively. Incubation with the secondary antibody was performed at 37°C for 20 min. After washing and mounting, specimens were analysed by conventional fluorescence microscopy as well as confocal laser scanning microscopy. For simultaneous visualization of chromosome domains and Sm antigen, *in situ* hybridization was followed by immunofluorescence procedures. Detection was achieved by dual colour fluorescence.

Confocal laser scanning microscopy

For three-dimensional analysis of fluorescently labelled specimen, confocal laser scanning microscopy (LSM 10, Zeiss, Germany) was applied. Following excitation with the 488 nm line of an argon ion laser and the 543 nm line of a helium neon laser, FITC and rhodamine/Texas red images, respectively, were acquired using a 63 × magnification (NA 1.4) oil immersion objective. The parameters of the instrument were chosen in a way that the fluorescent signals seen on the screen corresponded closely in shape and size to the fluorescent images seen by direct microscopic observation. Since thresholding applied to enhance the difference between a signal and background may change the shape and size of the digitized image of a chromosome domain, segmentations of domain borders were performed by two independent observers yielding very similar results.

Images of FITC and rhodamine (or Texas red) were taken in the same focal plane sequentially (< 5 sec between the acquisitions). There was no drifting of the object along the z-axis during the measurements. Following electronic overlaying, the geometrical relation of the FITC and rhodamine/Texas red signals was assessed. For illustration purposes, pictures were taken directly from the monitor.

Results

Cell type specific nuclear distribution of Sm antigens

In order to compare the distribution of splicing snRNPs in a variety of cell types, 10 different primary cell cultures and established cell lines were studied by

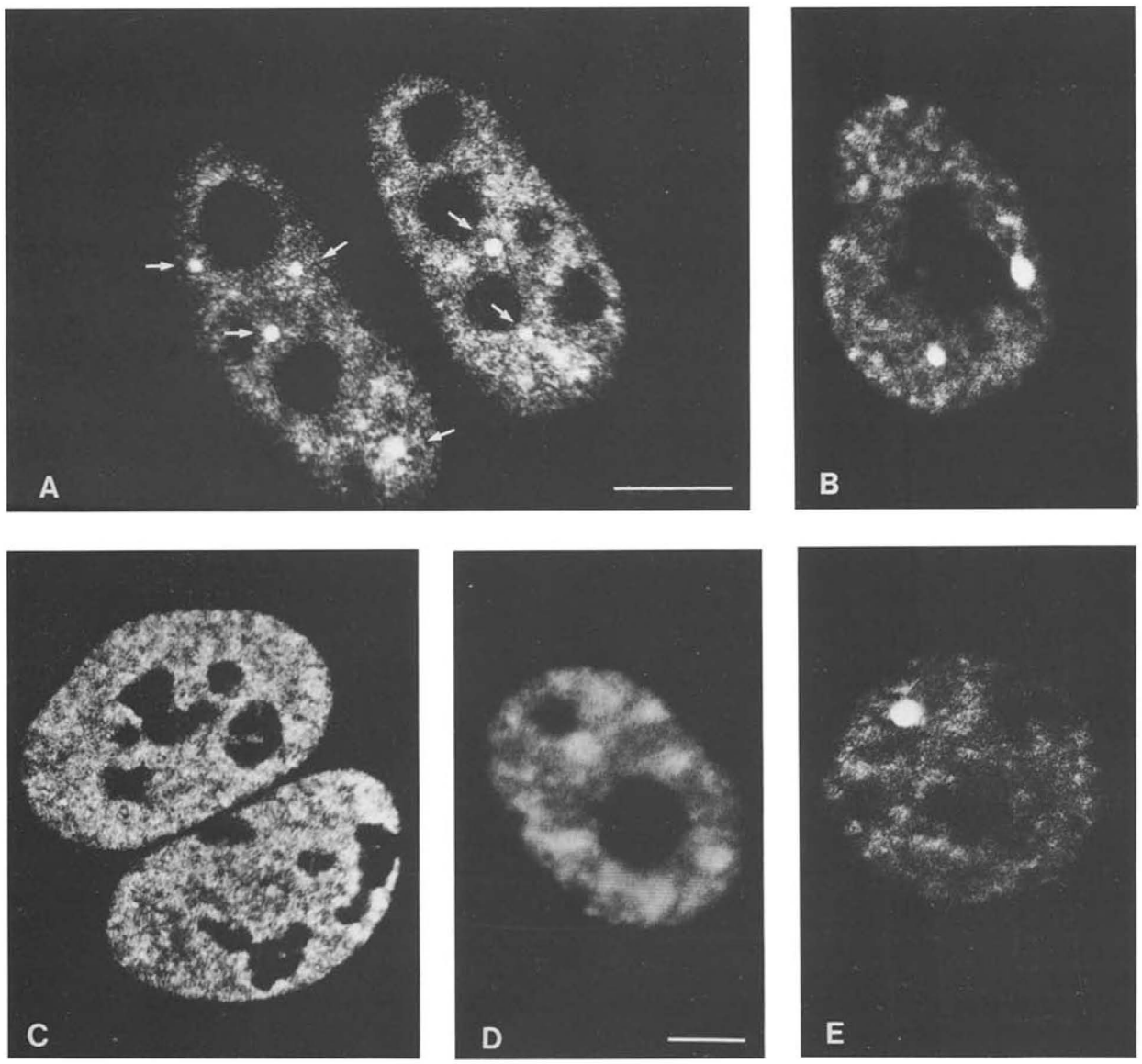

Figure 1. Specific Sm staining pattern in different types of cultured cells. Each panel represents an optical section obtained by confocal laser scanning microscopy. Incubation with the anti-Sm antibody Y12 results in all cell types in a staining throughout the nucleus excluding the nucleoli. **A**) HeLa cells display a fine grained staining with additional high focal concentrations (1–9 foci per cell). In this section four and two foci are visible in the left and right nucleus, respectively. **B**) Following 1 h heat shock, HeLa cells show fewer but enlarged foci, two of which are visible in this section (for details see text). **C**) Amniotic fluid cells display a dense, fine grained nuclear staining without foci. **D**) In CHO cells, the Sm antigen is localized in patches. **E**) The majority of HEL cells show only one large focus, as visualized in this section. Bar represents 10 μm.

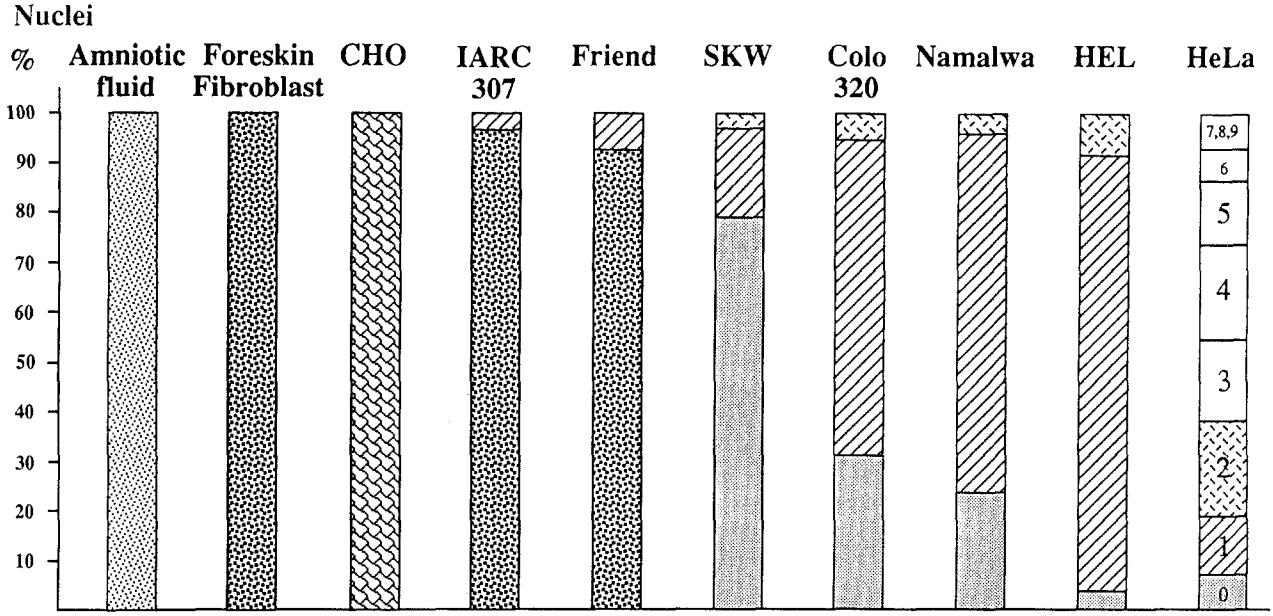

Figure 2. Quantitative description of the specific Sm staining pattern in different types of cultured cells. The nuclear staining by the Y-12 antibody was evaluated in 100-265 nuclei of each primary cell culture or established cell line. ▫, diffuse staining; ▩, disperse; ▩, speckled; ▩, in patches; ▨, one focus; ▨, two foci; □, more than two foci.

indirect immunofluorescence, using the monoclonal antibody Y12 directed against the Sm antigen. Cells were fixed in 4% paraformaldehyde, permeabilized with detergent, and incubated with anti-Sm antibodies. Following visualization by fluorochrome-conjugated antibodies, fluorescence microscopy revealed for each of the analysed cell cultures an overall nucleoplasmic staining pattern excluding the nucleoli (see Figure 1, 3A, 3D). Seven cell lines displayed additional, highly prominent local concentrations of Sm antigen (foci). The remaining three cell cultures, CHO cells, foreskin fibroblasts and amniotic fluid cells, displayed a patch-like (Figure 1D), punctate (speckled) (Figure 4 I,J) and disperse (Figure 1C) nuclear staining, respectively. As summarized in Figure 2, the number of foci varied both between and within cell cultures. IARC 307, Friend, SKW, Colo 320, Namalwa and HEL cell nuclei contained one or two Sm foci per cell. Of these, the lowest frequency of foci was found in IARC 307, with only 3% of the nuclei displaying one focus, whereas HEL-cells showed the highest frequency with 96% of the nuclei exhibiting one (88%) or two (8%) foci. In contrast, HeLa-cells contained 1–9 foci per nucleus (non-mitotic), with an average of 3 to 4 (Figure 1A). Notably, no Sm antigen focus was observed in any cell type during mitosis (see Figure 4H). Thus, the distribution of the essential splicing components clearly depends on the type of cultured cells.

In order to relate the coincidence of Sm foci and coiled bodies reported by others (see Introduction) to the different distributions of Sm antigen found in the present study, we simultaneously visualized the Sm and the coilin antigen by two-colour immunofluorescence. Data from the six cell types which were analysed in detail are summarized in Table 1. The two lines without focal Sm accumulations, amniotic fluid and CHO cells, did not show coiled bodies. In HEL cells foci of both antigens always coincided. In Friend, Namalwa and HeLa cells Sm foci always co-localized with coiled bodies, but some additional bodies were seen without Sm foci. The latter were always found within the nucleoli but in their periphery. Figure 3A–F, shows examples of confocal images of HeLa and Namalwa cell nuclei, where the nucleoplasmic coiled bodies co-localize with Sm foci, whereas the coiled bodies in the nucleoli do not reveal Sm accumulations (for possible explanations see Discussion).

Nuclear distribution of Sm antigen is altered upon heat shock

Heat shock of 45°C inhibits *in vitro* splicing (Bond 1988), results in redistribution of snRNP antigens (Spector *et al.* 1991), and disrupts the association of snRNPs and coiled bodies (Carmo-Fonseca *et al.* 1992). In order to analyse the influence of this physiological parameter on the nuclear distribution of snRNPs in further detail, we investigated the effect of mild and strong heat shock in two cell lines.

HeLa cells were maintained for different times at 42°C (mild heat shock). Immediately after this heat shock (hs) cells were fixed in 4% paraformaldehyde, permeabilized by detergent treatment and incubated with the anti-Sm antibody (Table 2). After 15 min at 42°C, no difference in the Sm antigen staining pattern

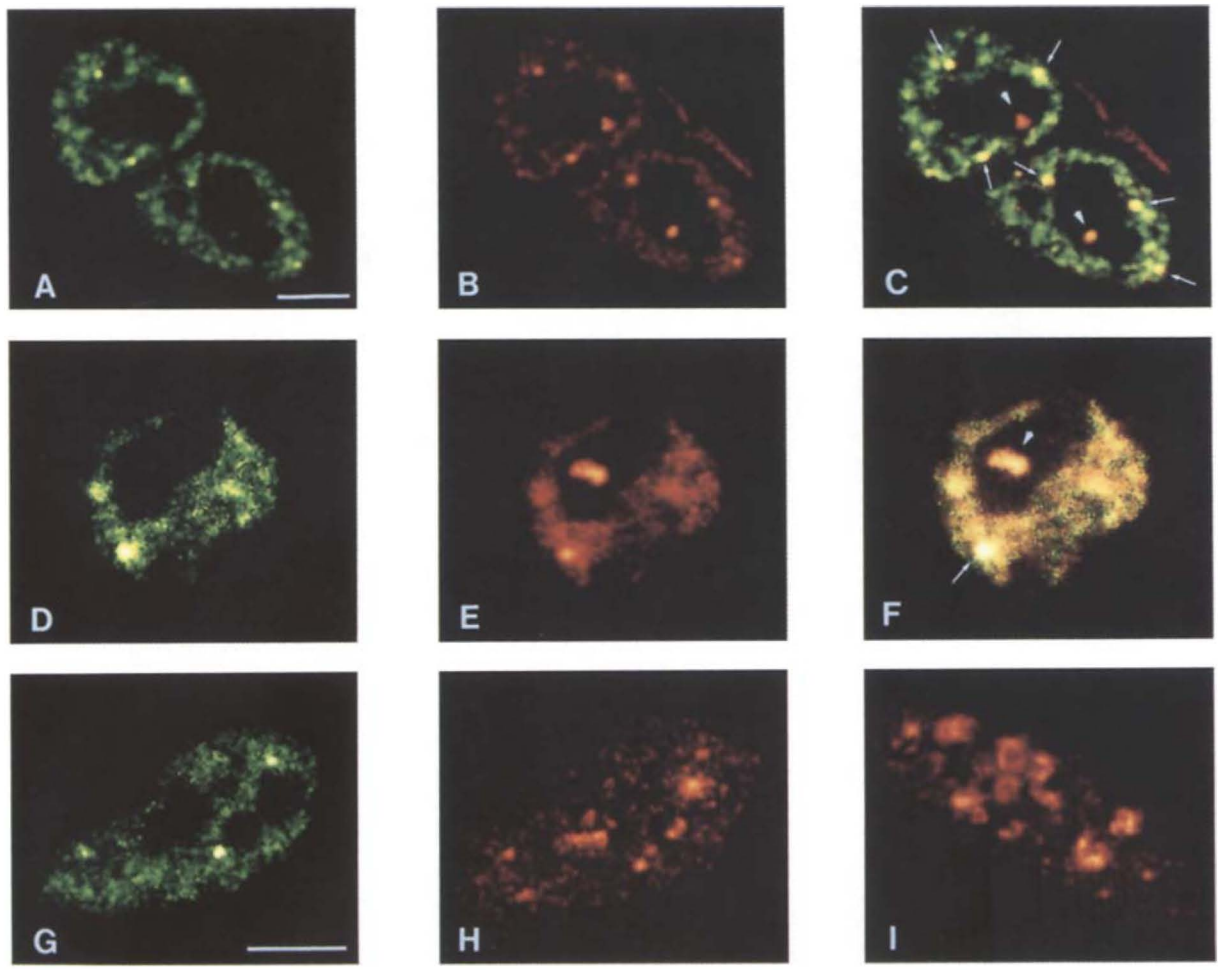

Figure 3. Two-colour immunofluorescence using anti-Sm (green) and anti-coilin (red) antibodies. Optical sections of A and B, as well as D and E are generated in the same focal planes. **A-C** Staining HeLa cell nuclei by the anti-coilin antibody (B), resembling the Sm-distribution (A), results in a general nuclear staining excluding the nucleoli and additional high focal concentrations, the coiled bodies. **C** An overlay of the two images exhibits co-localization of the snRNP foci and the coiled bodies (yellow, see arrows). However, some coiled bodies within or at the periphery of the nucleoli are not associated with Sm foci (green, arrowheads). **D–F** Staining of a Namalwa nucleus as in A, B, C. Whereas the Sm focus coincides with a coiled body, the nucleolar coiled body does not exhibit high concentrations of Sm antigen. **G,H** Immunofluorescence of a HeLa nucleus after 1 h heat shock at 42°C visualizing Sm antigen (G) and coilin (H). Note that despite the snRNP foci, the coilin concentrations look more like patches compared to the coiled bodies seen without heat shock (compare panel H with panels B and E) and desegregate from snRNP accumulation. Occasionally, these patches appeared as large 'doughnut-like' structures as shown in **I**. Bar represents 10 μm.

Figure 4. A–H (Opposite page) Simultaneous visualization of different chromosome domains and the Sm antigen in HeLa cells by a combination of *in situ* hybridization and indirect immunofluorescence. Each panel shows an optical section after overlaying digitized images from two different fluorochromes in the same focal plane. The chromosome domains (red) occur in areas which are excluded from the nuclear Sm staining (green). Examples are shown for chromosome 8 **(A-C** and **G, H)**, chromosome 7 **(D, E)** and chromosome 11 **(F)**. Note that the HeLa subline used in this study contains two normal chromosomes 8 and one additional smaller piece of chromosome 8 material. Note that Sm foci (some are indicated by arrows) are located at the border of, but not within, the domains. The more general Sm antigen staining could only occasionally be seen in areas of chromosomal domains (see panel **F**). The exclusive staining pattern was seen throughout the cell cycle, as seen with the highly condensed chromosomes prior to **(G)** and in mitosis **(H)**. Note, that during mitosis no focal accumulations of Sm antigen can be seen. **I, J** Primary human foreskin fibroblasts after hybridization with pBS 10 (panel **I**, red) or pBS 1 (panel **J**, red) and subsequent Sm staining (green). The anti-Sm antibody revealed a speckled nuclear staining. There is no overlap of speckles and areas occupied by a chromosomal domain. **K, L** HeLa cells were simultaneously hybridized with differentially labelled HPV cDNA (red) and the pBS 8 library (green) In **K** two larger RNA signals (see bigger arrows) are seen adjacent to the chromosome 8 domains. The additional smaller RNA signal (small arrow) cannot be related to a chromosome domain in this optical section, possibly because small additional chromosome 8 material was not detected with the pBS 8 probe. Both nuclei show that the HPV-RNA signal and the chromosome domains are closely associated but mutually exclusive (see higher magnifications in inlets). Bar represents 10 μm.

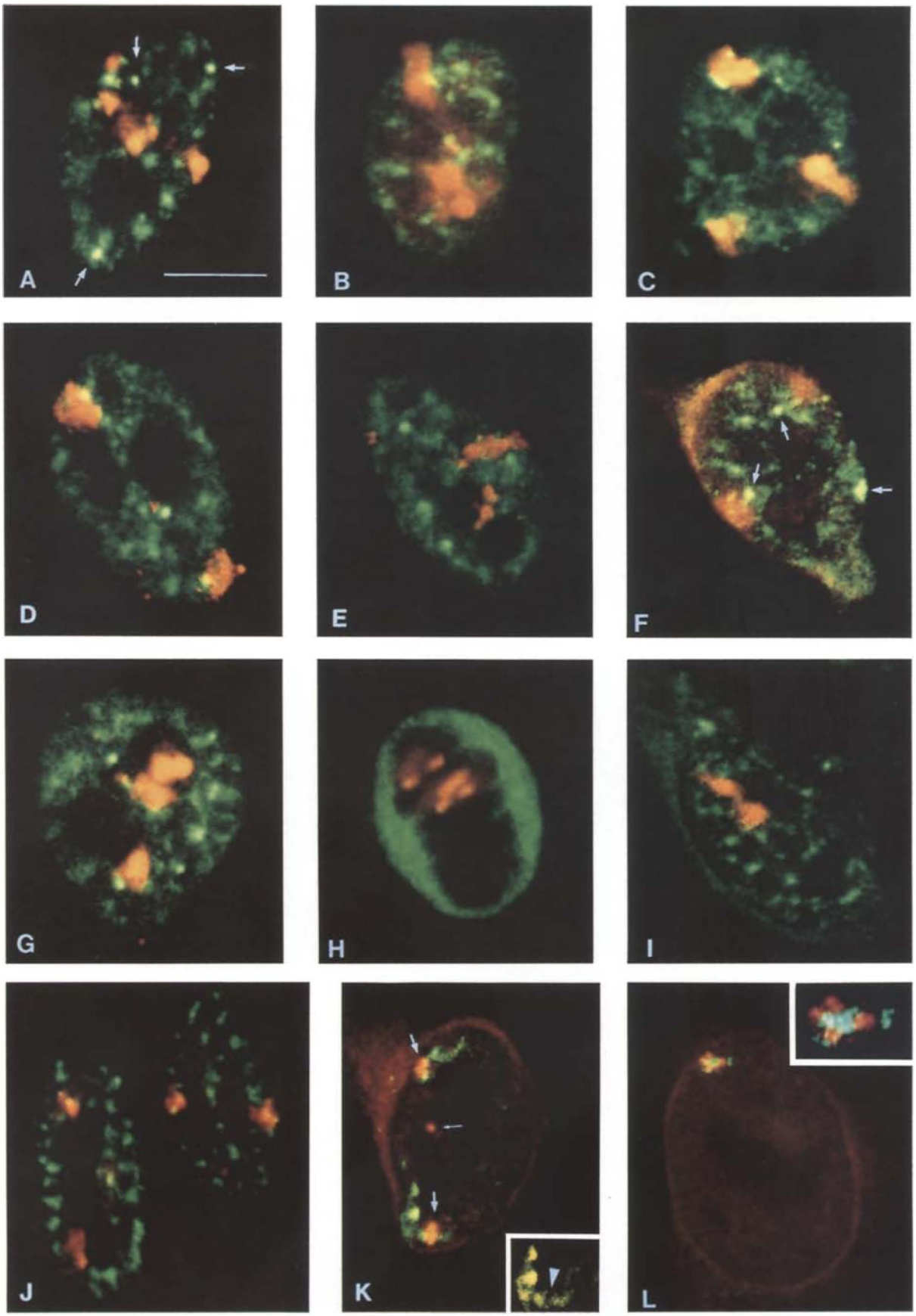
A
B
C
D
E
F
G
H
I
J
K
L

Table 1. Comparison of focal Sm accumulations and coiled bodies in various cell types

Cell type	Sm foci	Coiled bodies	All Sm foci co-localize with coiled bodies	Coiled bodies without Sm staining
Amniotic fluid	–	–	–	–
CHO	–	–	–	–
Friend	1	1–2	+	+
Namalwa	1–2	1–2	+	+
HeLa	1–9	1–9	+	+
HEL	1–2	1–2	+	–

was observed, whereas after 30 min the intensity of the nucleoplasmic staining clearly increased. Following 1 h heat shock, the shape and number of foci per nucleus changed (compare Figure 1, panels A & B). Two to four larger foci per nucleus were seen, and concomitantly the intensity of diffuse nuclear and cytoplasmic staining increased further. In order to quantitate these differences in foci dimension, 100 foci were measured each in cells with and without hs treatment. Without hs the foci had an average diameter of 0.90 μm (SD 0.15 μm), while the average size increased to 1.16 μm (SD 0.23 μm) after 1 h hs. This size difference was highly significant (unpaired t-test, $p < 0.0001$). Heat shock of 2 h or more resulted in bright disperse staining of nucleoplasm and cytoplasm, with no focal concentrations. In HEL cells the changes of Sm staining upon heat shock were similar to those seen in HeLa cells (see Table 2). However, no enlargement of foci could be observed after 30 min and foci had disappeared by 1 h after hs. When a stronger heat shock was applied (45°C) the apparent disintegration of Sm foci was accelerated in HeLa as well as in HEL cells (Table 2). It can be concluded that a mild hs has the same effect as a stronger hs, but the kinetics of the observed changes are increased at higher temperature.

Co-localization studies showed that Sm foci and coiled bodies desegregated during heat shock. One example is shown in Figure 3 (panels G and H). Furthermore, coiled bodies showed pronounced changes in morphology upon hs, with the appearance of doughnut-shaped bodies (Figure 3 panel I). This is in agreement with recent data indicating that the coiled body is a kinetic nuclear structure (Carmo-Fonseca *et al.* 1993).

Sm antigen foci are predominantly found on the surface of chromosome domains

The spatial relationships between chromosome domains and the subnuclear regions, where components of the mRNA processing pathway, are localized was investigated in two different cell types. HeLa cells and primary foreskin fibroblasts were subjected to fluorescence *in situ* hybridization of various DNA libraries established from sorted human chromosomes, followed by the immunodetection of Sm antigen using a different fluorochrome. The spatial relation of the labelled targets was assessed in optical sections applying confocal laser scanning microscopy.

The simultaneous visualization of chromosome domains and Sm antigen in the same focal plane revealed that both occupy generally exclusive areas (Figure 4A—H). The disperse nuclear distribution of Sm antigen in HeLa nuclei was only occasionally found to overlap with chromosomal DNA in the optical

Table 2. Changes in Sm distribution upon heat shock

Staining pattern	HeLa 42°C	HeLa 45°C	HeLa 42°C	HeLa 45°C
Distribution as under normal conditions (with foci)	15 min	–	15 min	–
Increase disperse nuclear staining (with foci)	30 min	15 min	30 min	15 min
Further increase in nucleoplasmic staining and enlarged foci	1 h	30 min	–	–
Bright disperse staining of nucleoplasm and cytoplasm, no foci	≥ 2 h	≥ 1 h	≥ 1 h	≥ 30 min

sections (Figure 4, panel F). Although limitations of the z-axis resolution of confocal microscopes have to be considered (see Discussion), the vast majority of optical sections revealed this exclusive occurrence. For a quantitative assessment, the relationships between the Sm foci and the painted chromosome domains were statistically analysed. In the optical section, where the highly concentrated Sm staining was in focus, digitized confocal images of the chromosome domain and the Sm staining were stored and electronically overlaid. The majority of Sm foci were not associated with the examined chromosome domain (ranging from 42% to 78%, not shown). The percentage of Sm foci in the areas of chromosome domains correlated well with the size and number of the domains (the HeLa line used in this study is highly aneuploid, but the material of the chromosomes analysed was previously characterized by various cytogenetic techniques). In HeLa cells this analysis was performed with the domains of chromosomes 1, 7, 8, 16, 18 and 20, evaluating more than 130 foci per chromosome. The spatial relationship was defined after inspection of overlaid images by two independent investigators. Two categories were defined: i) foci at the surface of the domain, when the centre of the focus was inside or outside the domain border by not more than the diameter of the focus (exterior area), and ii) foci within domains, ie. inside of the region defined as surface (interior area) (see Figure 5C). A high percentage of foci were located in the exterior area (Figure 5A). To distinguish whether foci are preferentially located in the exterior area or whether they are randomly associated with the chromosome domain, the size of exterior and interior areas was calculated for a series of chromosome domains in fibroblasts and HeLa cells segmented interactively by two independent investigators. For focal signals the exterior and interior areas were found to be roughly similar: 43% (exterior) versus 57% (interior) in fibroblasts, and 53% versus 47% in HeLa cells, respectively. A detailed description of the segmentation and evaluation procedures will be described elsewhere (A. Kurz *et al.* in preparation). Accordingly, if there is a random distribution of the focal signals within the painted chromosome domains one would expect roughly as many signals in the interior as in the exterior area. As shown in Figure 5A, our data clearly differ from a random distribution, with 93% (chromosome 7) to 98% (chromosome 16) of the Sm foci localized in the exterior and only 2% to 7% in the interior area. From these data it can be concluded that at least the snRNPs concentrated in foci are distributed at the surface of the chromosome domains.

A similar result was obtained for the distribution of Sm speckles and the domains of chromosome 1, 10 and 11 in human foreskin fibroblasts (see Figure 4 I and J). At least 110 domains were analysed per chromosome. Only a very low percentage of Sm speckles were located within a chromosome domain (8% for chromosome 1, 2% for chromosome 10 and 3% for chromosome 11), whereas the majority of the Sm accumulations were found in the exterior area (between 92% and 98%) (see Figure 5B).

Highly localized nuclear HPV-RNA is found in the periphery of the corresponding chromosome domains

HeLa cells contain a copy of the HPV18 genome integrated in chromosome 8 band q24. *In situ* hybridization with a cDNA probe of HPV18 allows the detection of the nuclear RNA transcripts. Control experiments including RNAse treatments and hybridization with and without denaturation of the target specimen allowed the unequivocal identification of the nuclear signals as a result of a hybridization to RNA, but not DNA, target sequences (data not shown). In accordance with the copy number of 8q24 in HeLa, three RNA signals were observed per nucleus (see Figure 4, K).

In order to analyse the spatial relationship between HPV18 RNA and the chromosome 8 domain, dual colour *in situ* hybridization was performed to simultaneously detect both nucleic acid targets, and confocal laser scanning microscopy was performed as above. Two examples are shown in Figure 4, K and L. Figure 6 summarizes the results obtained from 110 HPV signals. The majority of viral RNA signals (72%) were located at the surface of the domain. Furthermore, in 12% of the cases the signal was located in the domain, but further inspection revealed that the domain was only weakly stained at the site of the RNA signal. This may indicate an indentation of the domain surface at the site of the signal. Only 9% of HPV signals were found clearly within the domain by all criteria. Some signals could not be evaluated, because the chromosome domain was not visible when the HPV signal was in focus (2%) or because it was impossible to define the borders of the domain (5%).

Discussion

The different distribution patterns of Sm antigen described in this study contribute to the picture of cell type-specific differences in the shape and number of nuclear concentrations of splicing snRNPs (Carmo-Fonseca *et al.* 1991a, Spector *et al.* 1992). Focal accumulations were not seen in primary cell cultures established from human amniotic fluid cells and foreskin fibroblasts nor, in agreement with other reports (Spector 1990), in CHO cells. In our experiment, however, the latter showed a signal accumulation in patches rather than a speckled pattern of Sm staining. The speckled staining first described by Mattioli *et al.* (1971) and Northway & Tan (1972) was seen in the fibroblast, Friend and IARC 307 cell nuclei. Most of the analysed established cell lines exhibited snRNP foci.

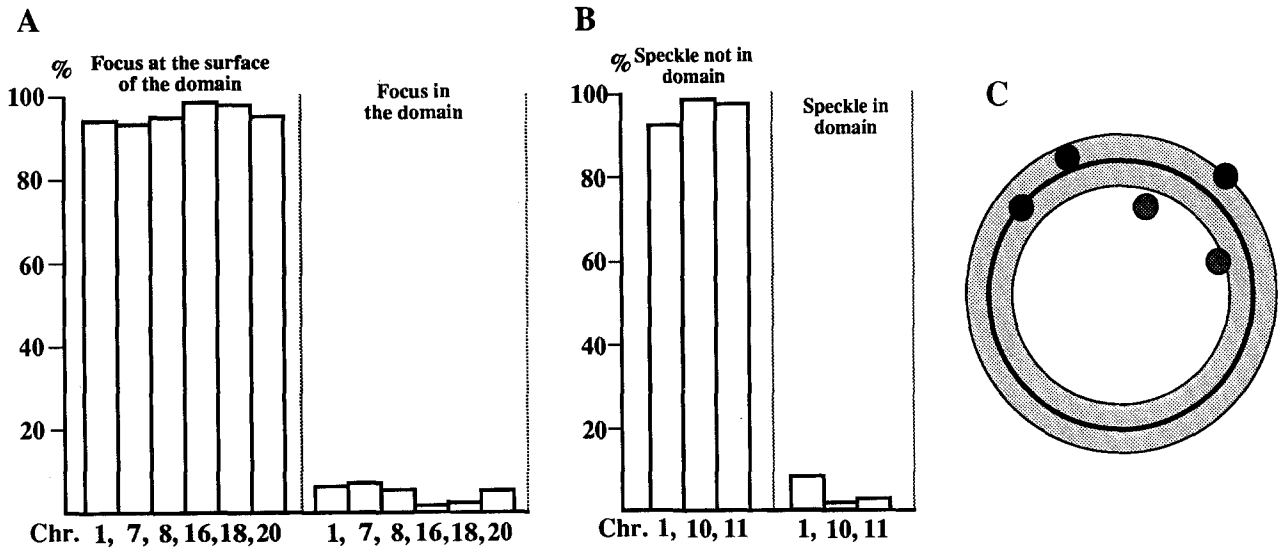

Figure 5. Spatial distribution of Sm foci in HeLa cells (**A**) and Sm speckles in primary human foreskin fibroblasts (**B**) with respect to chromosome domains. **C**) Schematic illustration of the interior and exterior area of a chromosome domain as outlined in the text. ▨, exterior area; □, interior area; ●, focus at the surface; ●, focus in the domain; ─, visible border of chromosome domain.

In HeLa cells the foci distribution was the same (1–9 foci) as previously reported (Carmo-Fonseca *et al.* 1991a), while several other lines showed only one prominent focus in the vast majority of cells.

The Sm foci have been described as concentrations of snRNPs in coiled bodies (Raska *et al.* 1991, Spector *et al.* 1992, Carmo-Fonseca *et al.* 1993). Accordingly, we found a co-localization of Sm and coilin antigen. However, in the present study additional coiled bodies were found within the nucleoli in which Sm antigen was not detectable. From the current data it cannot be excluded that this is due to a limited accessibility of the antibodies or a modification of the Sm epitope in these nucleolar coiled bodies. However, recent studies revealed that the coiled body is a kinetic structure (Carmo-Fonseca *et al.* 1993, Andrade *et al.* 1993) and the coiled bodies without detectable Sm staining might reflect a particular stage during the cycling interaction of snRNPs and coiled bodies. Recent experiments applying double fluorescent staining with the anti-coilin rabbit serum used in this study (raised against a coilin peptide) and human autoantibodies directed against coilin (kindly provided by Angus Lamond) showed again a staining of nucleolar coiled bodies only by the rabbit but not by the patient serum. Thus, it is also possible that the rabbit anti-coilin serum recognizes an additional epitope not related to coilin.

It has recently been found that snRNPs can separate from coiled bodies after certain treatments, such as inhibition of transcription (Carmo-Fonseca *et al.* 1992) or at lower temperature (Carmo-Fonseca *et al.* 1993) underlining the view of a cycling interaction. This is also confirmed by the desegregation of Sm foci and coiled bodies upon heat shock, as found in this study and by others (Carmo-Fonseca *et al.* 1992). Clearly, further investigations regarding co-localization of nuclear factors and the kinetics of these structures are needed to determine whether the focal accumulations of spliceosome components are the exclusive sites of pre-mRNA splicing, or whether they are areas of spliceosome storage and/or assembly (for a detailed discussion see Lamond & Carmo-Fonseca 1993). It will also be interesting to see how the data obtained for mammalian nuclei relate to the findings in amphibian oocyte nuclei, where snRNPs accumulate in at least three distinct types of granules, the so-called snurposomes (for review see Gall 1991).

The analysis of the spatial relationships of nuclear entities is technically demanding. Two problems need to be addressed in particular: i) the procedure for the visualization of nuclear components should cause as little damage to the nuclei as possible and not disrupt the relative position of the components, and ii) the optical detection system should allow resolution of different nuclear signals in three dimensions in order to reveal their spatial relationships. To optimize the conservation of the three-dimensional nuclear architecture in *in situ* hybridization experiments, we performed a series of experiments with varied fixation and permeabilization procedures using a number of different cell lines. The three-dimensional morphology was assessed by confocal laser scanning microscopy (our unpublished data). Best results were obtained with a modification of a procedure described by Manuelidis (1985) (see Methods).

High resolution optical sections through fluorescently labelled specimens can be obtained by applying deconvolutions to a series of images from consecutive sections acquired with a sensitive camera

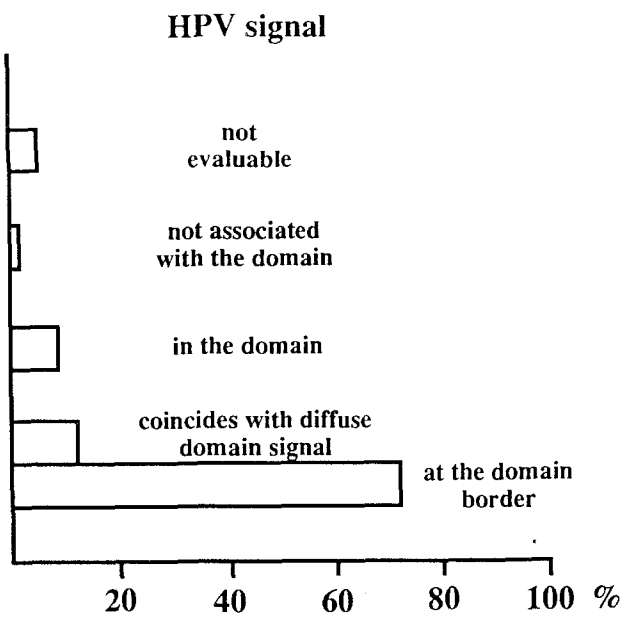

Figure 6. Spatial distribution of HPV 18-RNA with regard to the chromosome 8 domain in HeLa cells.

(Arndt-Jovin *et al.* 1985, Hiraoka 1987) or by sections generated with a laser scanning device in which out of focus fluorescence is reduced by means of a confocal diaphragm in the emission pathway (Cremer & Cremer 1978, Brakenhoff *et al.* 1979). In general, confocal microscopy yields a z-axis resolution of ≥ 0.5 µm, whereas the resolution in the x- and y-axes is about 0.2 µm (Jovin & Arndt-Jovin 1989, Shotton 1989, Van der Voort & Brakenhoff 1990). These numbers have to be taken into account when analysing the spatial relationships of two objects in the same focal plane by overlaying two separate images acquired by a confocal microscope. In the present study, this procedure was used to analyse the relationship between snRNPs and RNA transcript concentrations to chromosome domains. It might be argued that the overlaid fluorescence images do not resolve the labelled entities along the z-axis well enough to allow such a spatial assessment. However, the mutually exclusive localization of the analysed structures would be very difficult to explain by artefacts based on a limited z-axis resolution. New developments of axial tomography performed on a laser scanning microscope (Bradl *et al.* 1992) will help to elucidate further the spatial relation of labelled nuclear substructures. The high resolution in the x- and y-axes clearly allowed us to assess the localization of both the snRNPs and of the HPV-RNA at the surface of the chromosome domains in the overlaid images (see Figure 4).

As outlined in the Introduction, several kinds of nuclear domains have been described: nuclear domains defined by antigen accumulations, transcript domains defined by poly(A) accumulations, and chromosome domains defined by the territories occupied by individual chromosomes. We here report evidence not only for a mutually exclusive localization of these domains, but also for a specific occurrence of snRNPs and RNA transcripts at the surface of chromosome domains. On the basis of this previously unrevealed aspect of nuclear organization, we propose the model outlined below.

A model of the spatial organization of gene transcription and mRNA processing

We describe a model for a distinct nuclear compartment for gene transcription and RNA processing (see Figure 7). It is based on the finding that RNA transcripts and components of the splicing machinery are basically excluded from the interior of the territories occupied by the individual chromosomes. In other words, the chromosome domains on the one hand and the nuclear domains consisting of snRNPs and highly localized RNA transcripts on the other hand seem to be spatially exclusive. We postulate that the space between adjacent chromosome domains, including the surface areas of these domains, defines a structural and functional compartment, where nuclear components involved in transcription and mRNA processing are accumulated. This interchromosome domain (ICD) compartment would significantly reduce the volume where these components occur. This could facilitate the biochemical reactions involved in gene transcription and RNA processing, since the kinetics of a specific binding of two kinds of molecules is dependent on the concentration of the molecules in the reaction volume. The fact that the edges of the chromosome domains visualized by chromosome painting can be fuzzy is consistent with the assumption that decondensed DNA loops exist at the surface of the domains. Our model would allow for the coexistence of such looped DNA and the components of the transcription and splicing machinery in this nuclear compartment. This would fit with the well known decondensation of actively transcribed chromatin. The model implicates that transcribed genes are located in the periphery of the corresponding chromosome domains. This can be tested by means of multicolour *in situ* hybridization to visualize simultaneously individual genes and their respective chromosome domains. Preliminary data seem to support this view (A. Kurz & P. Lichter unpublished data).

The nuclear distribution of snRNPs as visualized by indirect immunohistochemistry has led to the assumption of a reticular network of snRNP throughout the nucleus (Spector 1990). This view could be integrated into the above model in the following way: it is known that snRNPs are co-localized with the coiled bodies, interchromatin granules and perichromatin fibrils. According to our model, all these structures are located in the ICD compartment as indicated in Figure 7. Depending on their density the distribution

of snRNPs could appear in a network-like manner. It is possible that the snRNPs do not provide an interconnected network *per se*, but are associated with other structural elements constituting such a network. At present it can only be speculated which networks exist or coexist in this space. However, since snRNPs and hnRNPs were shown to be associated with isolated nuclear matrix (for review see Berezney 1991) the possibility might be considered that at least part of the so-called non-chromatin matrix is present in this space. The model illustrated in Figure 7 can be tested rigorously, by analysing the spatial relation of chromosome domains and the growing number of transcription and splicing factors as exemplified in this study.

The association of perichromatin fibrils with RNA transcripts and the location of the latter at the surface of chromosome domains is consistent with our model: accordingly, genes should be preferentially transcribed in the decondensed region at the chromosome surface, and thus the RNA transcripts would be directly released in the ICD compartment. This is in accordance with the finding that RNA signals are spatially associated with the corresponding transcribed gene (Xing *et al.* 1993). The transport of the RNA to the pore complexes then would occur through the interchromosome domain space (possibly dependent on structures located in this space), explaining the sometimes track- or lane-like appearance of these RNA signals. The finding that accumulations of snRNPs coincide with poly(A) domains is compatible with our model, and it will be interesting to see how the regions detected by oligo(dT) probes and considered as transcript domains relate spatially to chromosome domains. The model presented here could, in principle, also be extended to other nuclear processes which could be spatially restricted to the interchromosome domain space.

Acknowledgements

We thank all the persons providing cells, DNA probes and antibodies (see Materials and Methods), Angus Lamond, Maria Carmo-Fonseca, Christoph Cremer and Patricia Emmerich for helpful discussions, Joachim Bradl for the assessment of chromosome domain parameters, and Michael Speicher for help with the statistical evaluation. This work was supported by a grant from the Deutsche Forschungsgemeinschaft (Li 406/2-1) and by the Verein zur Förderung der Krebsforschung in Deutschland.

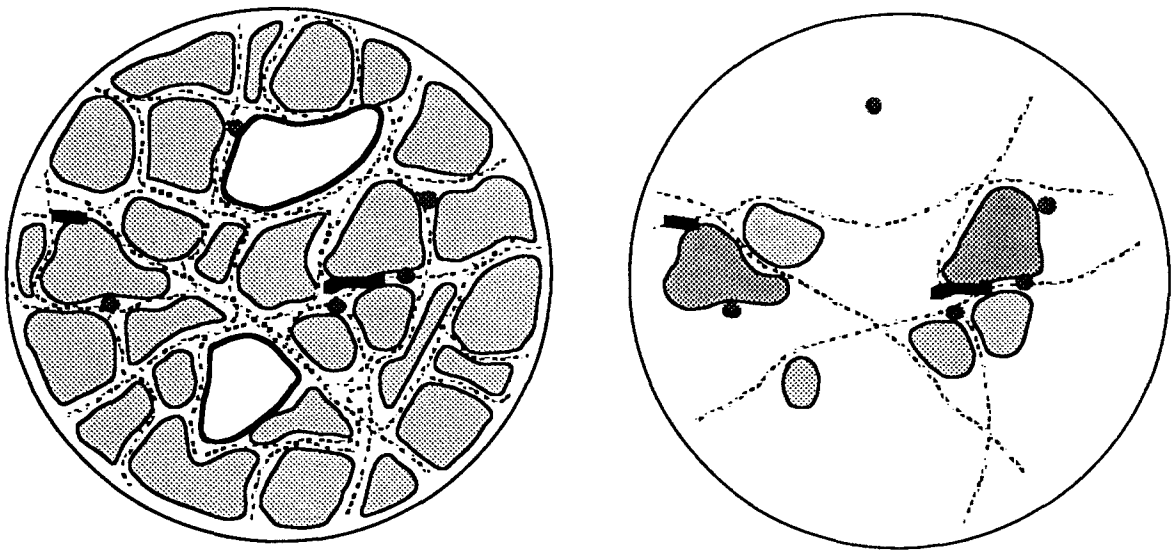

Figure 7. Schematic illustration of a model for the spatial organization of gene transcription and mRNA processing with regard to chromosome domains. For details see text. For illustration purposes the interchromosome domain space is augmented. Chromosome domain boundaries are indicated by lines, although the model allows for decondensed chromatin extending into the interchromosome domain space. For illustration purposes the accumulations of snRNPs are presented by only one character, although there are clear differences in e.g. speckles and foci. On the left half is a more comprehensive version of the model including all the chromosome domains of a particular optical section: on the right half is a scheme showing only selected parts of the model (e.g. three pairs of chromosome domains) in order to illustrate the spatial arrangements that could be expected after experiments visualizing selected nuclear components in multiple colours (part of the 'network' is shown here in addition). ◯, nucleolus; ◍, chromosome domain; •, high concentration of snRNPs ('foci' in coiled bodies or 'speckles'); ╲, highly localized nuclear RNA ('RNA-tracks', 'RNA-foci'); ╳, reticular structures containing for example perichromatin fibrils.

References

Andrade LEC, Tan EM, Chan EKL (1993) Immunocytochemical analysis of the coiled body in the cell cycle and during cell proliferation. *Proc Natl Acad Sci USA* **90**: 1947-1951.

Arndt-Jovin DJ, Robert-Nicoud M, Kaufman SJ, Jovin TM (1985) Fluorescence digital imaging microscopy in cell biology. *Science* **230**: 247-256.

Ascoli CA, Maul GG (1991) Identification of a novel nuclear domain. *J Cell Biol* **112**: 785-795.

Bachmann M, Mayet WJ, Schröder HC, Pfeifer K, Meyer zum Büschenfelde K-H, Müller WEG (1986) Association of La and Ro antigens with intracellular structures in HEp-2 carcinoma cells. *Proc Natl Acad Sci USA* **83**: 7770-7774.

Benyajati C, Worcel A (1976) Isolation, characterization, and structure of the folded interphase genome of *Drosophila melanogaster*. *Cell* **9**: 393-407.

Berezney R (1991) The nuclear matrix: A heuristic model for investigating genomic organization and function in the cell nucleus. *J Cell Biochem* **47**: 109-123.

Berman SA, Bursztajn S, Bowen B, Gilbert W (1990) Localization of an acetylcholine receptor intron to the nuclear membrane. *Science* **247**: 212-214.

Blobel G (1985) Gene gating: a hypothesis. *Proc Natl Acad Sci USA* **82**: 8527-8529.

Bond U (1988) Heat shock but not other stress inducers leads to the disruption of a sub-set of sn-RNPs and inhibition of *in vitro* splicing in HeLa cells. *EMBO J* **7**: 3509-3518.

Bouteille M, Laval M, Dupuy-Coin AM (1974) Localization of nuclear functions as revealed by ultrastructural autoradiography and cytochemistry. In: Busch H, ed. *The Cell Nucleus*. New York: Academic Press.

Bradl J, Hausmann M, Ehemann V, Komitowski D, Cremer C (1992) A tilting device for three-dimensional microscopy: application to *in situ* imaging of interphase cell nuclei. *J Microsc* **168**: 47-57.

Brakenhoff GJ, Blom P, Barends P (1979) Confocal scanning light microscopy with high aperture lenses. *J Microsc* **117**: 219-232.

Carmo-Fonseca M, Tollervey D, Pepperkok R, *et al.* (1991a) Mammalian nuclei contain foci which are highly enriched in components of the pre-mRNA splicing machinery. *EMBO J* **10**: 196-206.

Carmo-Fonseca M, Pepperkok R, Sproat BS, Ansorge W, Swanson MS, Lamond AI (1991b) *In vivo* detection of snRNP-rich organelles in the nuclei of mammalian cells. *EMBO J* **10**: 1863-1873.

Carmo-Fonseca M, Pepperkok R, Carvalho MT, Lamond AI (1992) Transcription-dependent colocalization of the U1, U2, U4/U6, and U5 snRNPs in coiled bodies. *J Cell Biol* **117**: 1-14.

Carmo-Fonseca M, Ferreira J, Lamond AI (1993) Assembly of snRNP-containing coiled bodies is regulated in interphase and mitosis—evidence that the coiled body is a kinetic nuclear structure. *J Cell Biol* **120**: 841-852.

Carter KC, Taneja KL, Lawrence JB (1991) Discrete nuclear domains of poly(A)RNA and their relationship to the functional organization of the nucleus. *J Cell Biol* **115**: 1191-1202.

Collins C, Kuo WL, Segraves R, Fuscoe J, Pinkel D, Gray J (1991) Construction and characterization of plasmid libraries enriched in sequences from single human chromosomes. *Genomics* **11**: 997-1006.

Comings DE (1980) Arrangement of chromatin in the nucleus. *Hum Genet* **53**: 131-143.

Cremer C, Cremer T (1978) Considerations on a laser-scanning-microscope with high resolution and depth of field. *Microsc Acta* **81**: 31-44.

Cremer T, Cremer C, Baumann H, *et al.* (1982) Rabl's model of the interphase chromosome arrangement tested in Chinese hamster cells by premature chromosome condensation and laser UV-microbeam experiments. *Hum Genet* **60**: 46-56.

Cremer T, Lichter P, Borden J, Ward DC, Manuelidis L (1988) Detection of chromosome aberrations in metaphase and interphase tumor cells by *in situ* hybridization using chro- mosome specific library probes. *Hum Genet* **80**: 235-246.

Fakan S, Leser G, Martin TE (1984) Ultrastructural distribution of nuclear ribonucleoproteins as visualized by immunocytochemistry on thin sections. *J Cell Biol* **98**: 358-363.

Fakan S, Leser G, Martin TE (1986) Immunoelectron microscope visualisation of nuclear ribonucleoprotein antigens within spread transcription complexes. *J Cell Biol* **103**: 1153-1157.

Gall JG (1991) Spliceosomes and snurposomes. *Science* **252**: 1499-1500.

Hiraoka Y, Sedat JW, Agard DA (1987) The use of a charge-coupled device for quantitative optical microscopy of biological structures. *Science* **238**: 36-41.

Hochstrasser M, Sedat JW (1987) Three-dimensional organization of *Drosophila melanogaster* interphase nuclei. II. Chromosome spatial organization and gene expression. *J Cell Biol* **104**: 1471-1482.

Huang S, Spector DL (1992) U1 and U2 small nuclear RNAs are present in nuclear speckles. *Proc Natl Acad Sci USA* **89**: 305-308.

Hutchison N, Weintraub H (1985) Localization of DNAse I-sensitive sequences to specific regions of interphase nuclei. *Cell* **43**: 471-482.

Jovin TM, Arndt-Jovin DJ (1989) Luminescence digital imaging microscopy. *Annu Rev Biophys & Biophys Chem* **18**: 271-308.

Lamond AI, Carmo-Fonseca M (1993) The coiled body. *Trends Cell Biol.*

Lawrence JB, Singer RH, Marselle LM (1989) Highly localized tracts of specific transcripts within interphase nuclei visualized by *in situ* hybridization. *Cell* **57**: 493-502.

Lerner EA, Lerner MR, Janeway JCA, Steitz JA (1981) Monoclonal antibodies to nucleic acid-containing cellular constituents: Probes for molecular biology and auto- immune disease. *Proc Nat Acad Sci USA,* **78**: 2737-2741.

Lichter P, Cremer T (1992) Chromosome analysis by non-isotopic *in situ* hybridization. In: Rooney DE, Czepulkowski BH, eds. *Human Cytogenetics*. New York: Oxford University Press.

Lichter P, Cremer T, Borden J, Manuelidis L, Ward DC (1988) Delineation of individual human chromosomes in metaphase and interphase cells by *in situ* suppression hybridization using recombinant DNA libraries. *Hum Genet* **80**: 224-234.

Lichter P, Tang CC, Call K, *et al.* (1990) High resolution mapping of human chromosome 11 by *in situ* hybridization with cosmid clones. *Science* **247**: 64-69.

Lichter P, Boyle AL, Cremer T, Ward DC (1991) Analysis of genes and chromosomes by non-isotopic *in situ* hybridization. *Genet Anal Tech Appl* **8**: 24-35.

Manuelidis L (1985) Individual interphase chromosome domains revealed by *in situ* hybridization. *Hum Genet* **71**: 288-293.

Manuelidis L (1985a) *In situ* detection of DNA sequences using biotinylated probes. *Focus* **7**: 4-8.

Manuelidis L (1990) A view of interphase chromosomes. *Science* **250**: 1533-1540.

Manuelidis L, Borden J (1988) Reproducible compartmentalization of individual chromosome domains in human CNS cells revealed by *in situ* hybridization and three-dimensional reconstruction. *Chromosoma* **96**: 397-410.

Mattioli M, Reichlin M (1971) Characterization of a soluble nuclear ribonucleoprotein antigen reactive with SLE sera. *J Immunol* **107**: 1281-1290.

Monneron A, Bernhard W (1969) Fine structural organization of the interphase nucleus in some mammalian cells. *J Ultrastructural Res* **27**: 266-288.

Northway JD, Tan EM (1972) Differentiation of antinuclear antibodies giving speckled staining pattern in immunofluorescence. *Clin Immunol Immunopathol* **1**: 140- 154

Nyman U, Hallman H, Hadlaczky G, Pettersson I, Sharp G, Ringertz NR (1986) Intranuclear localization of snRNP antigens. *Cell Biol* **102**: 137-144.

Paulson JR, Laemmli UK (1977) The structure of histone-depleted metaphase chromosomes. *Cell* **12**: 817-828.

Pinkel D, Straume T, Gray JW (1986) Cytogenetic analysis using quantitative, high sensitivity, fluorescence hybridization. *Proc Natl Acad Sci USA* **83**: 2934-2938.

Pinkel D, Landegent J, Collins C, *et al.* (1988) Fluorescence *in situ* hybridization with human chromosome-specific libraries: detection of trisomy 21 and translocations of chromosome 4. *Proc Natl Acad Sci USA* **85**: 9138-9142.

Raap AK, van de Rijke FM, Dirks RW, Sol CJ, Boom R, van der Ploeg M (1991) Bicolor fluorescence *in situ* hybridization to intron and exon mRNA sequences. *Exp Cell Res* **197**: 319-322.

Reuter R, Appel B, Bringmann P, Rinke J, Lührmann R (1984) 5'-terminal caps of snRNAs are reactive with antibodies specific for 2,2,7-trimethylguanosine in whole cells and nuclear matrices. *Exp Cell Res* **154**: 548-560.

Ramon y Cajal SR (1903) Un sencillo metodo de coloracion seletiva del reticulo protoplasmico y sus efectos en los diversos organos nerviosos de vertebrados y invertebrados. *Trab Lab Invest Biol* **2**: 129-221.

Raska I, Andrade LEC, Ochs RL, *et al.* (1991) Immunological and ultrastructural studies of the nuclear coiled body with autoimmune antibodies. *Exp Cell Res* **195**: 27-37.

Roggenbuck B, Larsen PM, Fey SJ, Bartsch D, Gissman L, Schwarz E (1991) Human papilloma virus type 18 E6*, E6, and E7 protein synthesis in cell-free translation systems and comparison of E6 and E7 *in vitro* translation products to proteins immunoprecipitated from human epithelial cells. *J Virol* **65**: 5068-5072.

Schardin M, Cremer T, Hager HD, Lang M (1985) Specific staining of human chromosomes in Chinese hamster × man hybrid cell lines demonstrates interphase chromosome territories. *Hum Genet* **71**: 281-287.

Schneider-Gädicke A, Schwarz E (1986) Different human cervical carcinoma cell show similar transcription patterns of human papilloma virus type 18 early genes. *EMBO J* **5**: 2285-2292.

Shotton DM (1989) Confocal scanning optical microscopy and its applications for biological specimens. *J Cell Sci* **94**: 175-206.

Spector DL (1984) Colocalization of U1 and U2 small nuclear RNPs by immunocytochemistry. *Biol Cell* **51**: 109-111.

Spector DL (1990) Higher order nuclear organization: three-dimensional distribution of small nuclear ribonucleoprotein particles. *Proc Natl Acad Sci USA* **87**: 147-151.

Spector DL, Lark G, Huang S (1992) Differences in snRNP localization between transformed and nontransformed cells. *Mol Biol Cell* **3**: 555-569.

Spector DL, Fu X-D, Maniatis T (1991) Associations between distinct pre-mRNA splicing components and the cell nucleus. *EMBO J* **10**: 3467-3481.

Spector DL, Schrier WH, Busch H (1983) Immunoelectron microscopic localization of snRNPs. *Biol Cell* **49**: 1-10.

Van der Voort HTM, Brakenhoff GJ (1990) 3-D image formation in high-aperture fluorescence confocal microscopy: a numerical analysis. *J Microsc* **158**: 43-54.

Verheijen R, Kuijpers H, Vooijs P, Van Venrooij W, Ramaekers F (1986) Distribution of the 70K RNA-associated protein during interphase and mitosis. *J Cell Sci* **86**: 173-190.

Xing Y, Lawrence JB (1991) Preservation of specific RNA distribution within the chromatin-depleted nuclear substructure demonstrated by *in situ* hybridization coupled with biochemical fractionation. *J Cell Biol* **112**: 1055-1063.

Xing Y, Johnson CV, Dobner PR, Lawrence JB (1993) Higher level organization of individual gene transcription and RNA splicing. *Science* **259**: 1326-1330.

Zorn C, Cremer C, Cremer T, Zimmer J (1979) Unscheduled DNA synthesis after partial UV irradiation of the cell nucleus. *Exp Cell Res* **124**: 111-119.